PNAS RESEARCH ARTICLE | NEUROSCIENCE

Transcytosis-mediated anterograde transport of TrkA receptors is necessary for sympathetic neuron development and function

Blaine Connor[a], Guillermo Moya-Alvarado[a], Naoya Yamashita[b], and Rejji Kuruvilla[a,1]

Edited by Rosalind Anne Segal, Dana-Farber Cancer Institute, Boston, MA; received March 28, 2022; accepted January 4, 2023 by Editorial Board Member Liqun Luo

In neurons, many membrane proteins, synthesized in cell bodies, must be efficiently delivered to axons to influence neuronal connectivity, synaptic communication, and repair. Previously, we found that axonal targeting of TrkA neurotrophin receptors in sympathetic neurons occurs via an atypical transport mechanism called transcytosis, which relies on TrkA interactions with PTP1B, a protein tyrosine phosphatase. Here, we generated TrkA^{R685A} mice, where TrkA receptor signaling is preserved, but its PTP1B-dependent transcytosis is disrupted to show that this mode of axonal transport is essential for sympathetic neuron development and autonomic function. TrkA^{R685A} mice have decreased axonal TrkA levels in vivo, loss of sympathetic neurons, and reduced innervation of targets. The neuron loss and diminished target innervation phenotypes are specifically restricted to the developmental period when sympathetic neurons are known to rely on the TrkA ligand, nerve growth factor, for trophic support. Postnatal TrkA^{R685A} mice exhibit reduced pupil size and eyelid ptosis, indicative of sympathetic dysfunction. Furthermore, we also observed a significant loss of TrkA-expressing nociceptive neurons in the dorsal root ganglia during development in TrkA^{R685A} mice, suggesting that transcytosis might be a general mechanism for axonal targeting of TrkA receptors. Together, these findings establish the necessity of transcytosis in supplying TrkA receptors to axons, specifically during development, and highlight the physiological relevance of this axon targeting mechanism in the nervous system.

axon transport | transcytosis | TrkA receptors | PTP1B tyrosine phosphatase | sympathetic neuron development

Significance

A fundamental question in the cell biology of neurons is how membrane proteins are targeted to axons after their biosynthesis in cell bodies. Axonal delivery of membrane proteins has been proposed to occur via several modes, including direct trafficking via the secretory pathway and transcytosis. Transcytosis is an atypical endocytosis-based mechanism, where newly synthesized proteins are first inserted on cell body surfaces, internalized, and anterogradely transported to axons. To date, information about transcytosis has been obtained from culture studies. However, how this mode of axon transport contributes to neuronal connectivity and function in vivo remains unknown. Using knock-in mice, we demonstrate that axonal delivery of neurotrophin receptors via transcytosis is essential for the development and function of sympathetic neurons.

The immense length of axons imposes unique challenges on neurons in that several proteins, synthesized in cell bodies, must be efficiently delivered to axon terminals. Many axonal membrane proteins with critical functions in regulating neuronal connectivity, synaptic transmission, and nerve repair are made in cell bodies that are meters away and need specialized mechanisms to be transported to their final destinations. Delivery of membrane proteins to axons, after biosynthesis in neuronal soma, has been proposed to occur via several modes, including direct delivery through the secretory pathway after sorting at the trans-Golgi network, nonpolarized delivery to axons and dendrites followed by selective retention in axons, or transcytosis where initial delivery of newly synthesized membrane proteins to somatodendritic compartments is followed by endocytosis and anterograde transport (1, 2). However, the functional contribution of each pathway to key processes in nervous system development, neurotransmission, and regeneration, and whether one mode of axonal transport is predominant at specific stages in the life of a neuron, remains as enduring questions in neuronal cell biology.

The family of tropomyosin-related kinase (Trk) receptors provides a prominent example of membrane proteins that undergo long-distance axonal trafficking to control neuronal survival, axon growth, and synaptic transmission (3, 4). In sympathetic and sensory neurons, axonal TrkA (Tropomyosin Receptor Kinase A) receptors are internalized after binding the ligand, nerve growth factor (NGF), secreted from peripheral tissues (5, 6). Axon-derived TrkA receptors are then retrogradely transported long distance to neuronal cell bodies/nuclei to exert transcriptional control of developmental programs (5, 6). The cellular and molecular mechanisms underlying retrograde TrkA trafficking are intensely investigated (3, 4, 7). However, relatively less is known about the anterograde trafficking of TrkA receptors to ensure continued responses to target-derived ligand.

Previously, we discovered that newly synthesized TrkA receptors are delivered to axons of sympathetic neurons by transcytosis (8, 9). Remarkably, in contrast to the constitutive secretory pathway, anterograde TrkA transcytosis is regulated by the ligand, NGF, acting on distal axons (9). Since NGF is a target-derived trophic factor for sympathetic neurons and is secreted in limiting amounts during development, regulated transcytosis suggests a positive feedback mechanism that serves to dynamically scale up receptor availability in axons at times of need.

Author contributions: B.C., G.M.-A., and N.Y. designed research; B.C. and G.M.-A. performed research; N.Y. contributed new reagents/analytic tools; B.C. and G.M.-A. analyzed data; and B.C. and R.K. wrote the paper.

The authors declare no competing interest.

This article is a PNAS Direct Submission. R.A.S. is a guest editor invited by the Editorial Board.

[1]To whom correspondence may be addressed. Email: rkuruvilla@jhu.edu.

This article contains supporting information online at https://www.pnas.org/lookup/suppl/doi:10.1073/pnas.2205426120/-/DCSupplemental.

Published February 2, 2023.

We uncovered the molecular underpinnings of ligand-induced transcytosis by showing that axon-derived TrkA receptors, retrogradely transported in response to NGF, are exocytosed to soma surfaces where they interact with naive resident receptors, resulting in their phosphorylation and internalization (9). Endocytosed TrkA receptors are then dephosphorylated by Protein Tyrosine Phosphatase 1B (PTP1B) (9), a protein tyrosine phosphatase anchored at the endoplasmic reticulum with its catalytic domain localized to the cytoplasmic face (10). Inhibition of PTP1B phosphatase activity in cell bodies of compartmentalized cultures of sympathetic neurons impairs TrkA transcytosis (9). In mice, sympathetic neuron-specific deletion of the PTP1B gene, *PTPN1*, results in neuron loss and impaired target innervation under limiting NGF ($NGF^{+/-}$) conditions (9). Together, these findings define PTP1B as a critical regulator of TrkA transcytosis and suggest a noncanonical role for a protein tyrosine phosphatase in positively regulating neurotrophin signaling by controlling receptor localization.

PTP1B has multiple substrates, including several receptor tyrosine kinases, adhesion factors, and endosomal proteins (10). Here, we generated $TrkA^{R685A}$ knock-in mice, where a point mutation in TrkA abolishes binding to PTP1B, to address the essential functions of PTP1B-mediated transcytosis of TrkA receptors in vivo. The $TrkA^{R685A}$ mice provide a specific genetic tool to dissect the functional outcomes of PTP1B-mediated TrkA trafficking in neurons without affecting other PTP1B substrates. We show that TrkA protein levels are drastically reduced in sympathetic axons innervating final target fields but not in ganglionic cell bodies in mutant mice, suggesting that transcytosis is a major mode for supplying TrkA receptors to axons in vivo. $TrkA^{R685A}$ mice exhibit sympathetic neuron loss and target innervation defects during development and dysautonomia. Thus, TrkA transcytosis mediated by PTP1B is a physiologically important mode of axonal targeting, with an essential role in sympathetic nervous system development and function.

Results

PTP1B-Dependent Transcytosis Is Necessary for Axonal Delivery of TrkA In Vivo. Trk receptors contain a conserved PTP1B substrate recognition motif (DYYR) in their tyrosine kinase activation domain (11, 12). Previously, we identified a point mutation (R685A) in the PTP1B recognition motif in the TrkA receptor that abolished PTP1B binding and prevented PTP1B-mediated TrkA dephosphorylation in sympathetic neurons (9). Notably, we found that the $TrkA^{R685A}$ point mutation impaired anterograde TrkA receptor transcytosis in compartmentalized cultures of sympathetic neurons (9). Since retrograde trafficking of axonal TrkA receptors to cell bodies is critical for NGF trophic signaling (3), we asked whether $TrkA^{R685A}$ receptors are capable of undergoing retrograde transport in sympathetic neurons. To visualize TrkA trafficking, we used a live-cell antibody feeding paradigm previously established in the laboratory (Fig. 1*A*) (8, 9). Compartmentalized sympathetic neuron cultures were infected with adenoviral vectors expressing FLAG-tagged chimeric receptors (FLAG-TrkB:A-WT or FLAG-TrkB:A-R685A) that have the extracellular domain of TrkB and transmembrane and intracellular domains of TrkA (9). Sympathetic neurons do not normally express TrkB receptors, and chimeric Trk receptors respond to the TrkB ligand, brain-derived neurotrophic factor (BDNF), but retain the signaling properties of TrkA (8). Surface chimeric receptors were live-labeled with anti-FLAG antibody exclusively in distal axon compartments. BDNF stimulation of axons (100 ng/mL, 20 min) resulted in robust internalization of FLAG antibody–bound TrkB:A-WT and FLAG-TrkB:A-R685A receptors in distal axons (Fig. 1 *B–F*). BDNF treatment of distal axons for a longer period (2 h) also resulted in the retrograde accumulation of both wild-type and mutant FLAG-labeled Trk receptors in cell bodies (Fig. 1 *G–K*). Together, these results indicate that axonal $TrkA^{R685A}$ receptors are able to internalize and be retrogradely trafficked in response to neurotrophin stimulation.

Encouraged by the results that $TrkA^{R685A}$ mutation specifically disrupts anterograde receptor transport (9), without affecting retrograde trafficking, we then decided to generate $TrkA^{R685A}$ knock-in mice to address the functional relevance of TrkA–PTP1B interactions in vivo. We used CRISPR/Cas9 technology to create the point mutation in the mouse *Ntrk1* gene (*SI Appendix*, Fig. S1 *A–E*). Founder homozygous mice were backcrossed to *C57BL/6* mice for at least three generations. Homozygous $TrkA^{R685A}$ mice survived to adulthood, were fertile, and had normal body weight at birth and as adults (*SI Appendix*, Fig. S1 *F* and *G*). Given that the $TrkA^{R685A}$ point mutation did not affect retrograde transport, we predicted that receptor kinase activity and downstream signaling should be preserved in the knock-in mice. To test this prediction, sympathetic neurons from neonatal $TrkA^{R685A}$ or $TrkA^{WT}$ mice were grown in mass cultures and stimulated with NGF (100 ng/mL) for 30 min. Neuronal lysates were immunoblotted for phosphorylated TrkA (P-TrkA) using an anti-phospho-TrkA antibody, P-$TrkA^{Y785}$ (PLC-γ1 binding site) (13), total TrkA, and the canonical downstream effectors, P-Akt and P-Erk1/2. NGF stimulation increased P-$TrkA^{Y785}$, P-Akt, and P-Erk1/2 levels in $TrkA^{R685A}$ neurons similar to $TrkA^{WT}$ cultures (Fig. 1 *L–O*). As an additional measure of TrkA activity, we asked whether the $TrkA^{R685A}$ mutation affects receptor phosphorylation at tyrosine residues, Y490 (Shc/FRS2 binding site) and Y674/675 (within the catalytic domain) (13). Immunoblotting of lysates prepared from the superior cervical ganglia (SCGs) of newborn $TrkA^{R685A}$ mice and control littermates with anti-phospho-TrkA antibodies, P-$TrkA^{Y490}$ and P-$TrkA^{Y674/675}$, revealed that mutant TrkA receptors were capable of being phosphorylated at these additional tyrosine residues to similar levels as wild-type receptors in sympathetic neuronal cell bodies in vivo (*SI Appendix*, Fig. S1 *H–K*). Together, these results indicate that disruption of TrkA–PTP1B binding does not interfere with receptor kinase activity and that mutant neurons retain their ability to respond to NGF.

To ask whether PTP1B-dependent transcytosis is an important means for delivering TrkA receptors to axons in vivo, we assessed TrkA protein levels in sympathetic nerve terminals in $TrkA^{R685A}$ mice. We performed immunoblotting for TrkA protein in salivary glands, a target tissue that is densely innervated by sympathetic axons from the SCGs, and neuron cell bodies in the SCGs in $TrkA^{R685A}$ mice and wild-type littermates. We performed this analysis in mice at embryonic day 16 (E16) when sympathetic axons are beginning to reach and innervate final target organs in response to target-derived NGF (6). Strikingly, the TrkA protein level in salivary glands of $TrkA^{R685A}$ embryos was only ~30% of that in wild-type animals, whereas the TrkA protein level in sympathetic ganglia was unaltered (Fig. 1 *P–S*). To ask whether the decrease was specific to TrkA receptors in mutant axons, we assessed the levels of the p75 neurotrophin receptor in sympathetic axons innervating salivary glands. In contrast to the reduction in TrkA protein levels, p75 protein levels were unaffected in $TrkA^{R685A}$ mutant axons (*SI Appendix*, Fig. S1 *L* and *M*). These results indicate that PTP1B-mediated TrkA transcytosis is a major mode of targeting TrkA receptors to sympathetic axon terminals.

Sympathetic Neuron Survival Is Compromised in $TrkA^{R685A}$ Mice. We next addressed the relevance of TrkA transcytosis in sympathetic neuron development in vivo. Tyrosine hydroxylase (TH) immunohistochemistry and quantification of cell numbers

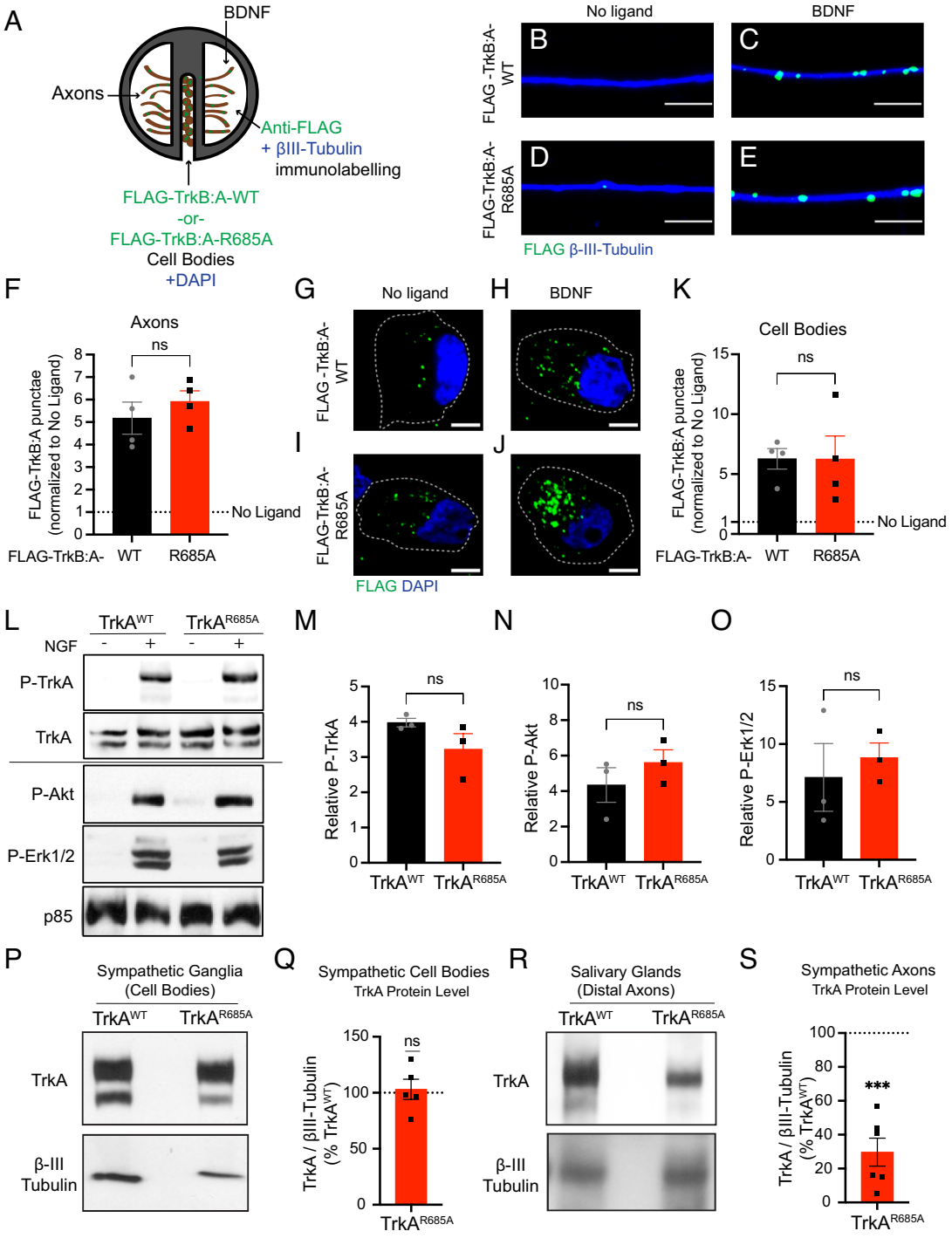

Fig. 1. Reduced axonal TrkA levels in TrkA^{R685A} sympathetic neurons. (*A*) Antibody feeding assay to monitor retrograde trafficking of axonal TrkA receptors. Sympathetic neurons, grown in compartmentalized cultures, were infected with adenoviral vectors for FLAG-TrkB:A-WT or FLAG-TrkB:A-R685A receptors. Distal axon compartments were live-labeled with FLAG antibody, followed by stimulation with BDNF (100 ng/mL) for 20 min or 2 h. (*B–E*) FLAG-TrkB:A-R685A receptors undergo ligand-induced internalization in axons, similar to FLAG-TrkB:A-WT receptors, after BDNF stimulation for 20 min. Axons were visualized by β-III-tubulin immunostaining. (Scale bar, 5 μm.) (*F*) Quantification of FLAG-Trk punctae in axons. Results are means ± SEM from four independent experiments and expressed as fold change relative to the "no ligand" condition. ns: not significant; *t* test. At least 10 axons per condition were assessed per experiment. (*G–J*) FLAG-TrkB:A-R685A receptors undergo retrograde transport to cell bodies, similar to FLAG-TrkB:A-WT receptors, after BDNF stimulation of distal axons for 2 h. Nuclei were labeled by DAPI (blue). (Scale bar, 5 μm.) (*K*) Quantification of FLAG-Trk punctae in axons. Results are means ± SEM from four independent experiments and expressed as fold change relative to the no ligand condition. ns: not significant; *t* test. At least 10 cell bodies per condition were assessed per experiment. (*L*) NGF stimulation (100 ng/mL, 30 min) promotes phosphorylation of TrkA, Akt, and Erk1/2 in mass cultures of TrkA^{R685A} and TrkA^{WT} sympathetic neurons, as assessed by immunoblotting. The P-TrkA blot was reprobed with TrkA for total receptor levels, while P-Akt and P-Erk1/2 blots were reprobed for p85 subunit of PI 3-kinase as a loading control. Solid line indicates samples run on different blots. (*M–O*) Quantification of P-TrkA, P-Akt, and P-Erk1/2 normalized to p85 levels. Results are means ± SEM from three independent experiments and expressed as fold change relative to the "no NGF" condition for each genotype. ns: not significant; *t* test. (*P–S*) TrkA protein levels are reduced in axons innervating salivary glands, but not in cell bodies in the SCGs, in TrkA^{R685A} embryos. SCGs (*P*) were harvested from E16 TrkA^{R685A} mice or TrkA^{WT} littermates, and lysates immunoblotted for TrkA. Immunoblots were stripped and reprobed for β-III-tubulin as a loading control. Salivary gland lysates (*R*), prepared from E16 TrkA^{R685A} mice or TrkA^{WT} littermates, were first subjected to TrkA immunoprecipitation and then immunoblotted for TrkA. Input lysates were immunoblotted for β-III-tubulin for protein normalization. Quantification of TrkA^{R685A} and TrkA^{WT} levels in SCGs (*Q*) and salivary glands (*S*) was normalized to β-III-tubulin. TrkA^{R685A} expression is represented as a % of the TrkA^{WT} levels. Results are means ± SEM from five to six mice per genotype. ***$P < 0.001$, *t* test.

by Nissl staining in tissue sections revealed no significant differences in the size of sympathetic ganglia (SCGs) and neuronal numbers between TrkA^{R685A} and wild-type embryos at E16 (Fig. 2 *A*–*C*). These results suggest that early developmental processes, including neuronal production, migration, and specification in the sympathetic nervous system, are unaffected in TrkA^{R685A} mice (6). However, by birth (P0), when sympathetic neurons are competing for limiting amounts of target-derived NGF for survival (6), we found a pronounced decrease in SCG size and neuronal numbers in TrkA^{R685A} pups (Fig. 2 *D*–*F*). These phenotypes were exacerbated

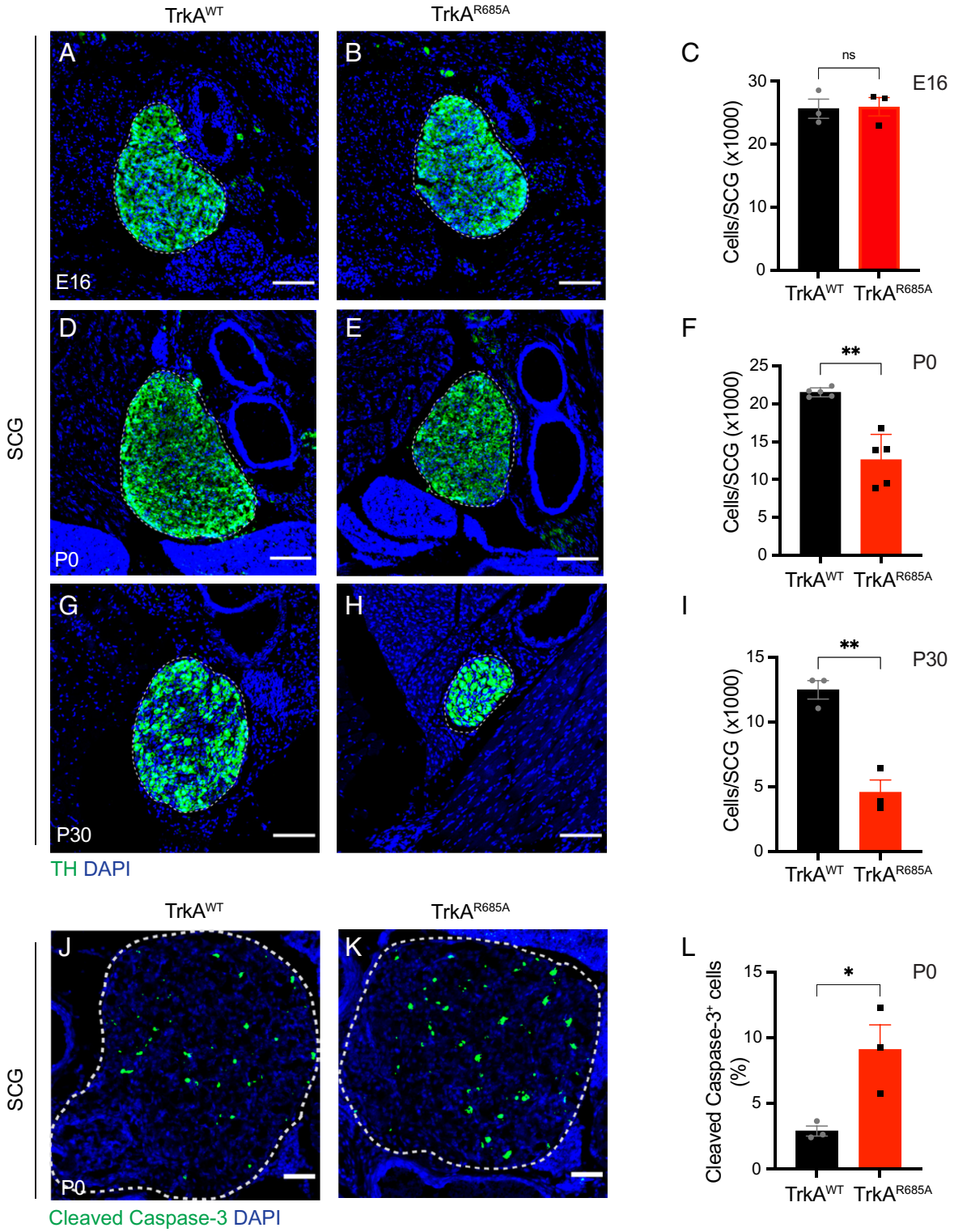

Fig. 2. Sympathetic neuron survival is compromised in TrkA^{R685A} mice. (*A*–*C*) Normal SCG size and neuron numbers in E16 TrkA^{R685A} mice. (*D*–*I*) Decreased SCG size and neuron numbers in newborn TrkA^{R685A} mice (*D*–*F*), which is exacerbated in P30 animals (*G*–*I*). SCGs were visualized by TH immunostaining. Nuclei are stained with DAPI (blue). Cell counts were performed on Nissl-stained SCG tissue sections. (Scale bar, 100 μm.) Results are means ± SEM from three to five mice per genotype. ns = not significant, $^{**}P < 0.01$, *t* test. (*J*–*L*) Increased apoptosis in SCGs from P0 TrkA^{R685A} mice assessed by cleaved caspase-3 immunostaining (green). Nuclei are stained with DAPI (blue), and SCGs are outlined by dashed line. (Scale bar, 50 μm.) Cleaved caspase-3–positive cells are expressed as a % of total SCG numbers. Results are means ± SEM from three mice per genotype. $^{*}P < 0.05$, *t* test.

by 4 wk after birth (P30) (Fig. 2 *G–I*) but did not progress any further in adult mutant mice analyzed at 4 mo of age (P120). Specifically, quantification of SCG neuronal numbers revealed a substantial 41.4% decrease in P0 TrkA^{R685A} mice (12,620 ± 1,500 neurons in TrkA^{R685A} mice versus 21,520 ± 263 in control littermates). The depletion of SCG neurons continued postnatally in TrkA^{R685A} mice, with P30 mutant mice exhibiting marked neuronal loss (62% decrease) compared to wild-type littermates (4,750 ± 953 neurons in TrkA^{R685A} mice versus 12,480 ± 716 in control littermates). However, neuronal loss was not any further exacerbated in 4-mo-old mutant mice (7,077 ± 1,272 neurons in TrkA^{R685A} mice versus 13,040 ± 1,951 neurons in control littermates at P120) (*SI Appendix*, Fig. S2 *A–C*). Neuronal loss in TrkA^{R685A} mice is primarily due to enhanced apoptosis since we found a significant threefold increase in apoptotic cells in mutant ganglia at P0 as revealed by cleaved caspase-3 immunostaining (Fig. 2 *J–L*) and TUNEL (*SI Appendix*, Fig. S2 *D–F*). Immunolabeling for Ki67 indicated that cell proliferation was unaffected in TrkA^{R685A} mutant ganglia at P0 (*SI Appendix*, Fig. S2 *G–I*). Together, these results indicate that PTP1B-mediated TrkA transcytosis is required for sympathetic neuron survival during the developmental period of NGF dependence.

In the peripheral nervous system, small-diameter nociceptive neurons in the dorsal root ganglia (DRGs) express TrkA and require NGF for survival during development (14). To ask whether PTP1B-mediated transcytosis is important for other NGF-responsive neurons in addition to sympathetic neurons, we assessed the number of TrkA-positive DRG neurons using immunohistochemistry and neuronal cell counts in TrkA^{R685A} mice and control littermates. We found a significant depletion (38% decrease) of TrkA-positive DRG neurons in TrkA mutant mice compared to control littermates at birth (2,717 ± 35 neurons in TrkA^{R685A} mice versus 4,393 ± 10 in control littermates) (*SI Appendix*, Fig. S2 *J–L*). These results suggest that transcytosis is required for the development of additional TrkA-expressing neuronal populations.

Axon Innervation Defects in TrkA^{R685A} Mice. Given that NGF also supports developmental axon growth, we next assessed sympathetic axon innervation of distal target fields using TH immunostaining. We observed decreased innervation in several SCG targets, including salivary glands, the olfactory epithelium, and the eye, in TrkA^{R685A} embryos at E16 (Fig. 3 *A–I*), a time when there is no neuronal loss in the ganglia (Fig. 2 *A–C*). The target innervation defects persist and are aggravated at postnatal stages P0 and P30 in the mutant animals compared to control littermates (Fig. 3 *J–L* and *SI Appendix*, Fig. S3 *A–C*), suggesting that the reduced innervation does not reflect a developmental delay but rather represents the failure of sympathetic axons to grow into end organs in response to target-derived NGF. However, in older TrkA^{R685A} mutant animals at 4 mo of age, the axonal innervation deficit was not any further exacerbated compared to 1-mo-old animals (*SI Appendix*, Fig. S3 *D–F*) similar to our observations that there was no progressive loss of mutant neurons after 1 mo (*SI Appendix*, Fig. S2 *A–C*). Together, these results suggest that TrkA transcytosis is predominantly required during a developmental period when sympathetic neurons are critically dependent on target-derived NGF for survival and growth.

Since TH expression is known to be regulated by TrkA signaling (15), we also assessed target innervation by immunostaining for Tuj1 (β-III-tubulin), a pan-axonal marker. We observed decreased Tuj1 immunoreactivity in E16 TrkA^{R685A} salivary glands compared to control tissues (*SI Appendix*, Fig. S3 *G–I*), although this effect was not as severe as the decrease in TH immunoreactivity. This is likely due to sympathetic nerves constituting a fraction of total peripheral innervation.

Together, these results suggest that anterograde TrkA delivery via transcytosis is necessary for sympathetic axon growth and target innervation in vivo. Since the defects in target innervation precede the neuronal loss in TrkA^{R685A} mice, these results suggest that axon growth is more sensitive than neuronal survival to disruptions in axonal TrkA levels. The neuronal loss may reflect the failure of sympathetic axons to gain access to adequate levels of target-derived NGF because of the diminished innervation and reduced neuronal responsiveness as axonal TrkA receptors get depleted over time.

TrkA^{R685A} Neurons Show Reduced Survival and Growth in Response to NGF. To directly address whether the developmental phenotypes in TrkA^{R685A} mice reflected attenuated neuronal responsiveness to target-derived NGF, we tested the ability of mutant neurons to grow and survive in response to axon-applied NGF in compartmentalized cultures. NGF (30 ng/mL) added only to distal axons promotes robust growth in TrkA^{WT} neurons, with an average growth rate of ~90 μm per day (Fig. 4 *A*, *B*, and *E*). In contrast, the growth-promoting effect of NGF was abolished in TrkA^{R685A} neurons (Fig. 4 *C*, *D*, and *E*), with neurites showing retraction and degeneration. In axon growth assays, the broad-spectrum caspase inhibitor, boc-aspartyl(O-methyl)-fluoromethyl ketone (BAF, 50 μM), was added to cell bodies of compartmentalized cultures so that axon growth could be assessed independent of complications of apoptosis.

We also monitored neuronal survival in response to NGF (30 ng/mL) added to distal axons in compartmentalized cultures of TrkA^{R685A} or TrkA^{WT} neurons. NGF was sufficient to support the survival of the majority of TrkA^{WT} neurons with only 9 ± 2% neurons undergoing apoptosis when assessed by cleaved caspase-3 immunostaining after 3 d of NGF treatment of distal axons (Fig. 4 *F*, *G*, and *J*). In contrast, TrkA^{R685A} neurons exhibited a significant increase in neuronal apoptosis (75 ± 3.4% apoptotic neurons), despite the presence of NGF on distal axons (Fig. 4 *H* and *J*). Thus, although TrkA^{R685A} receptors were capable of undergoing retrograde transport when acutely stimulated with ligand on distal axons for 2 h (Fig. 1 *G–K*), mutant neurons showed reduced survival in response to NGF long term (after 3 d in culture), likely due to the gradual diminution of TrkA receptors in axons over time. NGF added directly to neuronal cell bodies in compartmentalized cultures is capable of promoting neuronal survival (16, 17). Notably, in this condition, TrkA^{R685A} neurons were viable and healthy (8.85 ± 1.1% apoptotic neurons) (Fig. 4 *I* and *J*), consistent with our earlier findings that the point mutation does not disrupt overall receptor signaling capacity (Fig. 1 *L–O*). Together, these findings suggest that TrkA^{R685A} neurons specifically show reduced responsiveness to the NGF ligand when it is present on distal axons because of the depleted receptor levels in axons.

Autonomic Defects in TrkA^{R685A} Mice. Sympathetic neurons regulate diverse physiological processes to maintain body homeostasis under basal conditions or to mobilize "fight-or-flight" responses to danger or stress (6). Given the neuron loss and target innervation defects in neonatal TrkA^{R685A} mice, we asked whether autonomic responses were impacted in adult mutant mice at 6 to 8 wk of age. Loss of sympathetic innervation to the eye results in ptosis, or eyelid droop, in knockout mice lacking NGF or TrkA (18, 19) and is also observed in humans with Horner's disease (20) or familial dysautonomia (21). Strikingly, TrkA^{R685A} mice had prominent ptosis compared to wild-type littermates (Fig. 5 *A–C*), suggesting that TrkA transcytosis is critical for establishing the proper sympathetic neuron connectivity necessary for autonomic functions.

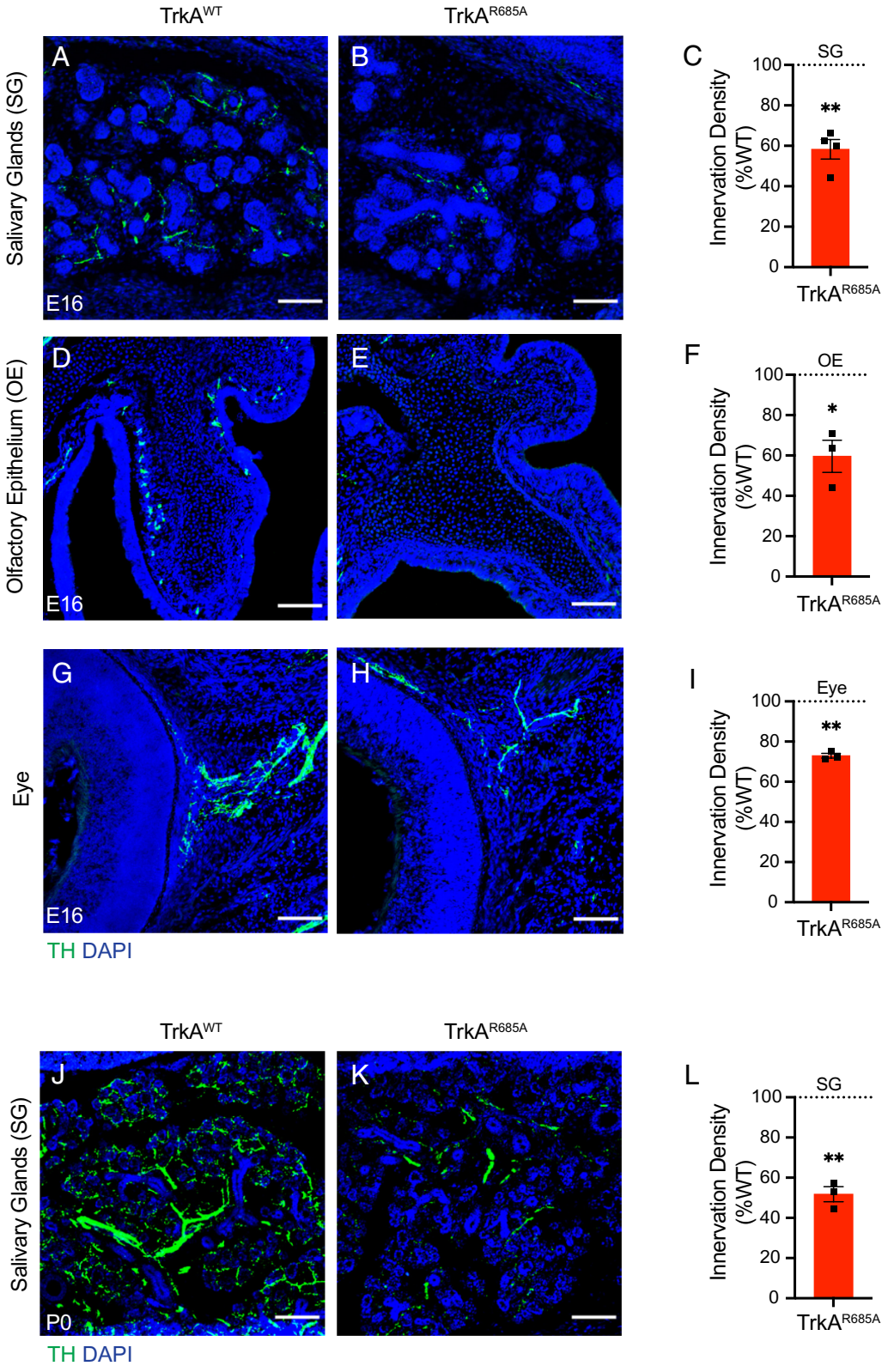

Fig. 3. Reduced axon innervation of sympathetic targets in TrkA^{R685A} mice. (*A–I*) TH immunostaining of salivary glands (*A–C*), the olfactory epithelium (*D–F*), and the eye (*G–I*) reveals diminished sympathetic axon innervation in targets in E16 TrkA^{R685A} mice compared to littermate controls. (*J–L*) Further depletion of innervation in salivary glands by birth in TrkA^{R685A} mice revealed by TH immunostaining. Nuclei are stained with DAPI (blue). (Scale bar, 100 μm.) (*C*, *F*, *I*, and *L*) Quantification of TH-positive sympathetic nerves by measuring integrated fluorescence densities per unit area using ImageJ. Results are mean ± SEM from three to four mice per genotype and represented as a % of TrkA^{WT} values. *P < 0.05, **P < 0.01, one-sample t test with hypothetical mean of 100%.

As another assessment of sympathetic activity, we measured pupil area in mutant and control mice. In mammals, pupil size can serve as a noninvasive and rapid readout for autonomic function (22). Pupil size is modulated by a balance of sympathetic versus parasympathetic activity, with the sympathetic component regulating pupil dilation, while parasympathetic activity controls pupil constriction (22). To measure basal pupil size, control and TrkA^{R685A} mice were dark-adapted for 2 d, and pupil sizes recorded

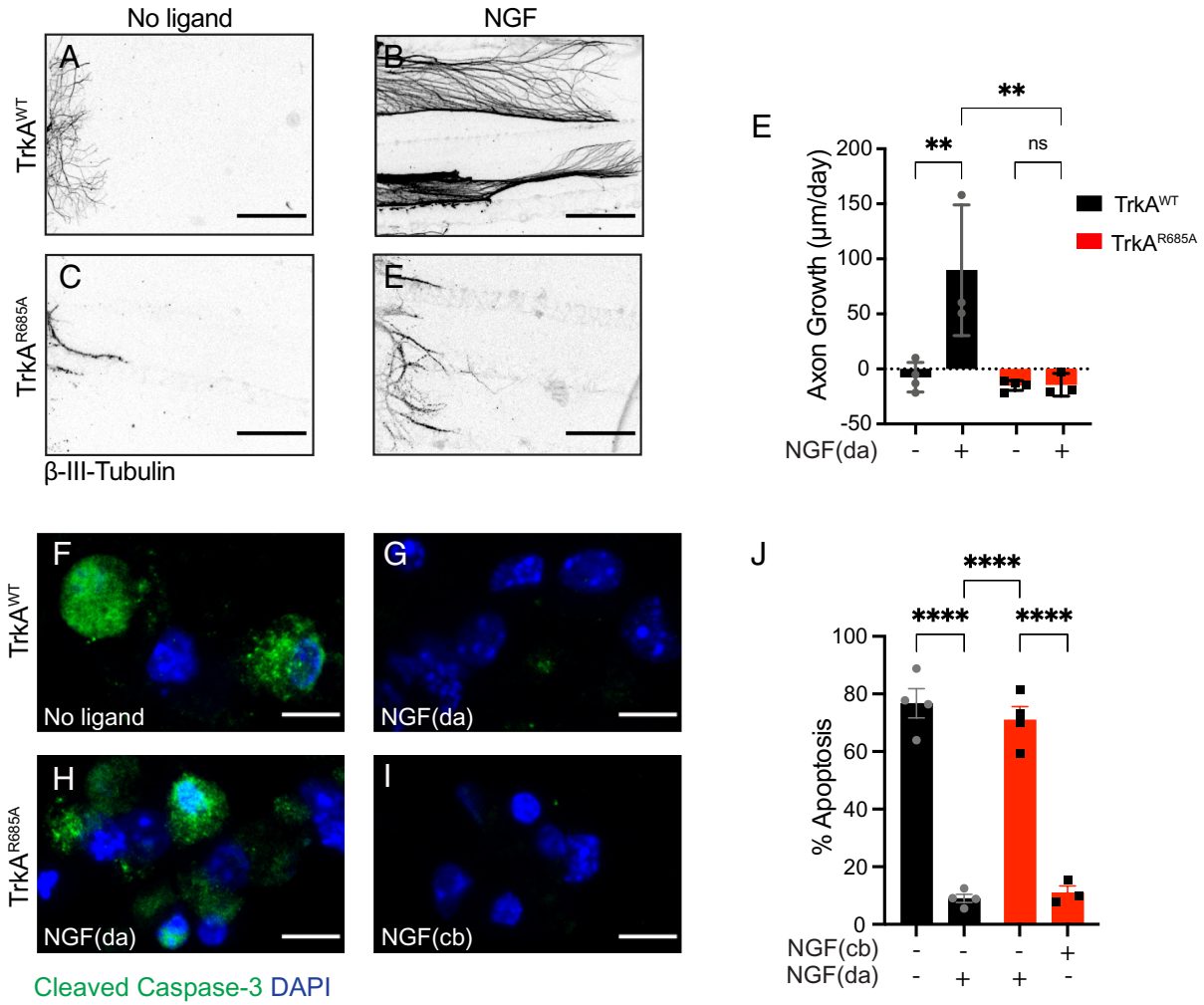

Fig. 4. Impaired NGF-dependent axon growth and neuron survival in TrkA^{R685A} neurons. (*A–D*) NGF-dependent axon growth is abolished in TrkA^{R685A} neurons. Compartmentalized cultures of sympathetic neurons from P0-P3 TrkA^{R685A} or TrkA^{WT} mice were either deprived of NGF by including anti-NGF in media bathing both cell body and axon compartments (*A* and *C*) or maintained with NGF (30 ng/mL) added solely to distal axon compartments (*B* and *D*). The caspase inhibitor, BAF (50 μm), was included in all analyses to prevent cell death. Panels are representative images of axons immunostained with anti-β-III-tubulin at the end of the analyses. (Scale bar, 360 μm.) (*E*) Quantification of rate of axon growth (μm/d assessed in 24-h intervals for a total of 72 h). Results are means ± SEM from three to four independent experiments. At least 10 to 15 axons per condition per experiment were analyzed. $^{**}P < 0.01$, two-way ANOVA and Tukey–Kramer post hoc test. (*F* and *G*) NGF (30 ng/mL) added only to distal axons (da) promotes survival of TrkA^{WT} neurons compared to the no ligand condition, as assessed by cleaved caspase-3 immunostaining. (*H* and *I*) Neuronal survival is compromised in TrkA^{R685A} neurons when NGF (30 ng/mL) is present on distal axons (da) but not when NGF is added directly to cell bodies (cb). Neuronal nuclei were labeled with DAPI (blue). (Scale bar, 5 μm.) (*J*) Quantification of neuronal apoptosis by determining the percentage of neurons that were cleaved caspase-3 positive. Only neurons that had extended axons into side chambers, defined by the retrograde accumulation of fluorescent microspheres, were scored for apoptosis. Results are means ± SEM from three independent experiments. At least 20 neurons per condition were assessed per experiment. Two-sample *t* test with multiple comparisons and Tukey–Kramer post hoc test, $^{****}P < 0.0001$.

for 30 s in the dark in unanesthetized mice (23). We found that TrkA^{R685A} mice showed a pronounced decrease in basal pupil area compared to control mice (Fig. 5 *D–F*). To ask whether this phenotype is due to increased parasympathetic activity, we measured pupil constriction in response to increasing light intensities, ranging from 0.01 to 1,000 lux, administered for 30 s. Light onset at 0.01 lux or higher resulted in rapid constriction with greater constrictions at higher light intensities in both TrkA^{R685A} mice and control mice (*SI Appendix*, Fig. S4). The intensity response curves were virtually identical for the two groups (*SI Appendix*, Fig. S4). These results suggest that parasympathetic function is intact in TrkA^{R685A} mice and that the smaller pupil areas likely reflect a decrease in sympathetic tone.

Discussion

In this study, using a newly generated knock-in mouse model, we describe the in vivo relevance of transcytosis-mediated axonal delivery of TrkA receptors in sympathetic neuron connectivity and function. We show that a point mutation in the TrkA receptor, which disrupts TrkA transcytosis by preventing receptor interactions with PTP1B, elicits a marked depletion of TrkA protein from sympathetic axons, profound neuronal loss, reduced axon innervation of target tissues, and dysautonomia in mice. These results provide evidence that transcytosis is a key mode of targeting TrkA receptors to sympathetic axons to support neural development in response to target-derived NGF and for subsequent autonomic function.

It is striking that a point mutation in the TrkA receptor elicits robust phenotypes during sympathetic nervous system development that mimic several of the defects observed in mice with global deletion of the TrkA receptor (24). For example, by birth, TrkA^{R685A} mice show a 41% decrease in SCG neurons close to the magnitude of the 50% neuron loss observed in TrkA$^{-/-}$ mice (24). Similarly, both TrkA^{R685A} and TrkA$^{-/-}$ mice also show reduced axon innervation of sympathetic target tissues starting at embryonic stages (~E16.5) (24). In contrast to the TrkA$^{-/-}$ mice, we provide

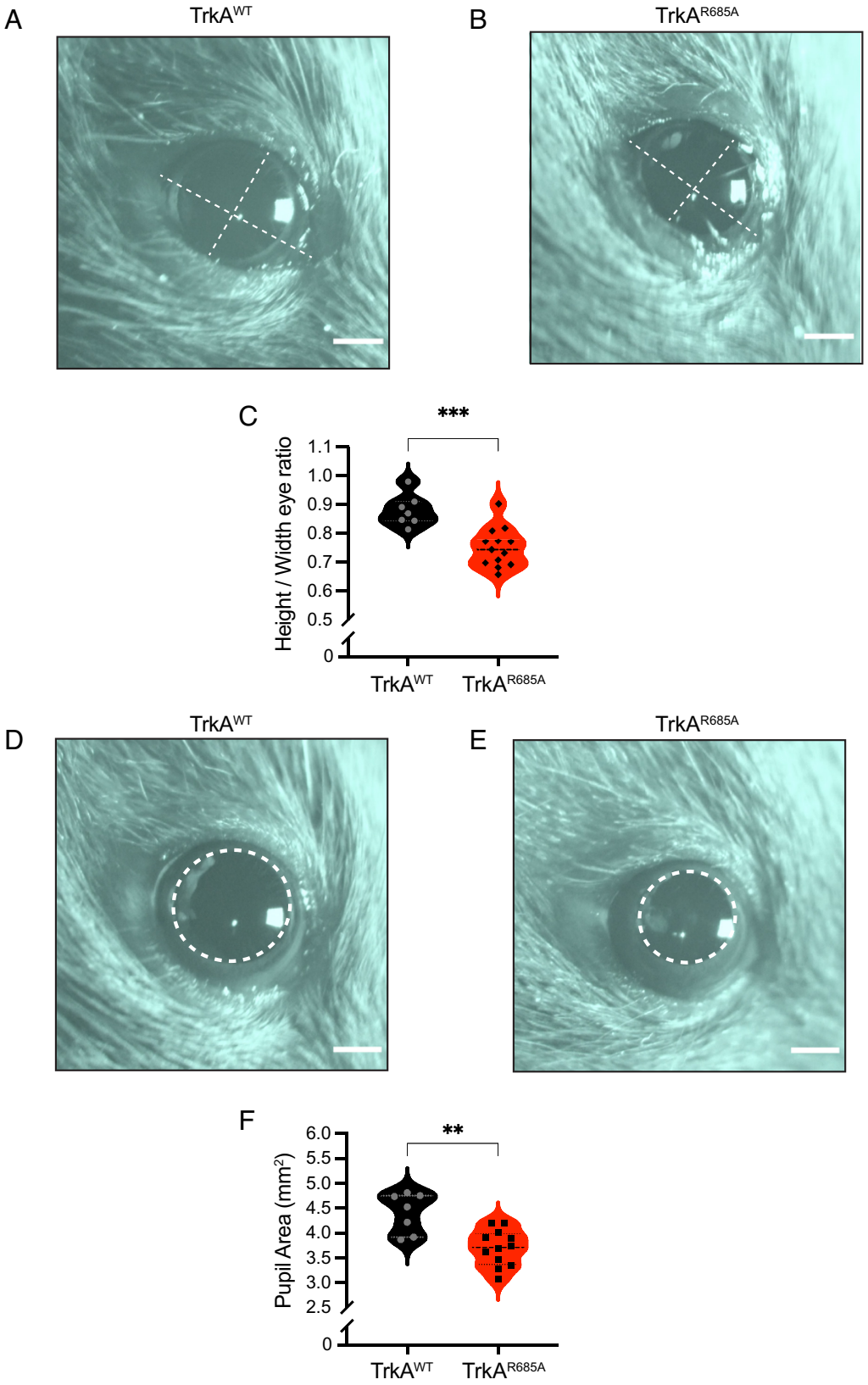

Fig. 5. Autonomic defects in TrkA^{R685A} mice. (*A* and *B*) Representative images of ptosis (eyelid droop) in adult TrkA^{R685A} mice compared to those in littermate controls. Dashed lines indicate height and width of the eye. (Scale bar, 1 mm.) (*C*) Quantification of ptosis (ratio of height over width of the eye). Results are the mean ± SEM from 13 TrkA^{R685A} and 7 TrkA^{WT} mice. ***$P < 0.001$, *t* test. (*D* and *E*) Dark-adapted TrkA^{R685A} mice have decreased basal pupil size compared to control littermates. Pupil is outlined in dashed lines. (Scale bar, 1 mm.) (*F*) Quantification of pupil area. Results are presented as mean ± SEM from 13 TrkA^{R685A} and 7 TrkA^{WT} mice. **$P < 0.01$, *t* test.

evidence, however, that the TrkA^{R685A} mutation elicits profound sympathetic abnormalities in the absence of any disruptions in receptor kinase activity, downstream signaling, or expression in ganglionic cell bodies. The most prominent cellular defect in TrkA^{R685A} neurons is the depletion of axonal TrkA receptors, which compromises neuronal responsiveness to target-derived ligand.

Together, with our previous findings (9), we conclude that perturbed axonal targeting of TrkA receptors through transcytosis underlies the defects in sympathetic neuron development. Given that adult TrkA^{R685A} mice are viable, in contrast to TrkA$^{-/-}$ mice, we were also able to perform physiological analyses to show that maintenance of axonal TrkA levels is critical for autonomic behaviors.

The robust sympathetic neuron phenotypes in TrkA^{R685A} mice were particularly surprising given our previous findings that conditional deletion of PTP1B did not result in overt deficits in sympathetic neuron survival or axon innervation of targets in mice (9). In PTP1B knockout sympathetic neurons, we observed a significant and specific depletion in axonal TrkA levels (9) similar to our findings in TrkA^{R685A} knock-in mice in this study. However, survival and innervation defects in PTP1B conditional knockout mice were only unmasked upon NGF haploinsufficiency (*NGF*$^{+/-}$) mice (9). One possible explanation is that since PTP1B dephosphorylates multiple substrates (10), up-regulated tyrosine phosphorylation of one or more of these substrates could have neurotrophic effects that counter the detrimental effects of impaired TrkA targeting in PTP1B knockout mice. Thus, the TrkA^{R685A} knock-in mice provide a more precise genetic tool to dissect the interactions of PTP1B with TrkA, leaving its role in other signaling pathways intact, and affording a unique molecular handle to study the role of transcytosis in neuron development. In defining a role for PTP1B in promoting NGF-dependent trophic functions through controlling axonal localization of TrkA receptors, our findings expand the canonical view that protein tyrosine phosphatases typically diminish signaling responses to extracellular signals (25, 26).

Our findings raise the possibility that different modes of axonal targeting may be utilized during distinct stages of sympathetic nervous system development. Trk receptors can be anterogradely transported to axons via the secretory pathway (27–30). Therefore, constitutive delivery via the direct secretory pathway might serve to deliver TrkA receptors to growing sympathetic axons during the initial phases of axon outgrowth and extension along intermediate vascular targets, which are NGF independent (6). However, when sympathetic axons reach final NGF-expressing targets, PTP1B-mediated TrkA transcytosis might be a mechanism to amplify neuronal responsiveness during a developmental competition for limiting amounts of target-derived ligand. Consistent with this notion, in TrkA^{R685A} mice, we observed attenuated innervation of end organs and loss of postmitotic sympathetic neurons during the developmental period of known dependence on NGF trophic signaling, which extends from late embryonic stages to first 3 to 4 wk after birth in mice (31, 32). Notably, we found that neuronal loss and blunted innervation were not significantly exacerbated in 4-mo-old TrkA mutant animals compared to 1-mo-old animals. These results suggest that once neuronal connectivity is established with target tissues, disruptions in transcytosis did not elicit further deficits in neuronal or axonal viability. Together, these findings suggest that secretory transport and transcytosis likely act in a sequential manner to meet the dynamic needs of neurons during development and maturation.

Our results suggest that transcytosis might be a general mechanism for axonal targeting of TrkA receptors in NGF-responsive neuronal populations since we observed a significant loss of TrkA-expressing nociceptive neurons in the DRGs during development in TrkA^{R685A} mice. The importance of TrkA receptor transcytosis in the trophic support of neurons may also extend beyond development. In the brain, basal forebrain cholinergic neurons that mediate memory and attention are known to be particularly susceptible to degeneration in Alzheimer's disease (33, 34). It would be of interest in future studies to assess the role of aberrant TrkA receptor transcytosis in disease pathogenesis.

Materials and Methods

Details of key resources are provided in *SI Appendix, Key Resources Table*.

Experimental Model and Subject Details.

Animals. All procedures relating to animal care and treatment conformed to the Johns Hopkins University Animal Care and Use Committee and NIH guidelines. Male and female mice were included in all experiments. Mice were housed under standard conditions with access to food and water ad libitum. Pregnant Sprague Dawley rats were purchased from Taconic Biosciences. Dissociated cultures of sympathetic neurons were established from SCGs harvested from P0 to P1 rat pups of both sexes as previously described (35).

Neuronal cultures. Sympathetic neurons were harvested from P0 to P1 Sprague Dawley rats or P0 to P4 TrkA^{R685A} or TrkA^{WT} mice, enzymatically dissociated, and grown in mass cultures or compartmentalized cultures as described previously (17, 36). Cells were maintained in culture with high-glucose Dulbecco's Modified Eagle Medium (DMEM) supplemented with 10% fetal bovine serum (FBS), penicillin/streptomycin (1 U/mL), and NGF purified from mouse submaxillary glands (100 ng/mL) (37). For NGF deprivation, neurons were placed in high-glucose DMEM containing 1.0% FBS with anti-NGF (1:1,000) and BAF (50 μM) for 36 h. For adenoviral infections, neuronal cultures were infected with high-titer CsCl-purified or VivaPure AdenoPack20-purified pAdenoX-Tet3G adenoviruses for 36 h as previously described (9). Adenovirus-mediated protein expression was induced by adding doxycycline (Sigma, 100 ng/mL) to culture media.

Method Details.

Generation of TrkA^{R685A} knock-in mice. TrkA^{R685A} knock-in mice were generated using the CRISPR/Cas9 technology. CHOPCHOP (38) and DESKGEN CRISPR (39) softwares were used to identify guide RNA target sites. *Ntrk1* sequence was obtained from the University California Santa Cruz (UCSC) genome browser for the mm10 database (Genome Reference Consortium m38.81 assembly). crispr RNA (cRNA) guide sequences within 50 base pairs of the desired mutation site, an on-target activity score above 45% (40), a protospacer length of 20 nucleotides, and NGG protospacer-adjacent motif (PAM) were initially selected. The sequences were scored for off-target activity (41). The selected sequence, 5′-AAGGTTTAGGGACACTTACTCGG-3′, generated an activity score of 46% and a specificity score of 86% (40, 41). The crRNA was synthesized by Dharmacon, and the tracrRNA and Cas9 protein were provided by the Johns Hopkins University (JHU) Transgenic Core Facility. A single-stranded DNA oligonucleotide (ssODN) template with 50-base pair homology arms flanking 5′-TGCC-3′ was designed as the homology-directed repair (HDR) template. The HDR template was designed based on Ntrk1 transcript NM_001033124.1 (-) using Edit-R HDR Donor Designer software from Horizon Discovery. To prevent Cas9-mediated cleavage following the repair, the third nucleotide of the PAM recognition sequence was silently mutated (C → T), preserving the tyrosine residue in the resulting amino acid sequence and generating a BceAI restriction enzyme site. The HDR template was synthesized by Dharmacon, with phosphorothioate linkages between the terminal nucleotides for added stability and increased functionality. The JHU Transgenic Core performed pronuclear injections and implantation into C57BL/6J pseudopregnant females to generate TrkA^{R685A} knock-in animals. Founder mice positive for the *TrkA^{R685A}* allele were identified by PCR amplification, Sanger sequencing, and restriction fragment length polymorphism (RFLP) analysis using BceAI restriction enzyme and backcrossed with C57BL/6J mice for at least three generations prior to experimental analyses. Colonies were maintained by mating heterozygous mice to generate knock-in homozygous mice, knock-in heterozygous mice, and littermate wild-type mice. PCR genotyping was done using a common forward TrkA primer (5′-TCTCTCTGTCTCCGTCTTTCT-3′) and reverse primer sequences for the TrkA^{WT} allele (5′-AGGTTTAGGGACACTTACTCGG-3′) or TrkA^{R685A} allele (5′-AGGTTTAGGGACACTTACGGCA-3′). For RFLP analysis, the following primers were used: a forward primer (5′-CCTAGTCTCTTCCTTCCTCAAATC-3′) and a reverse primer (5′-CCAGAGCTCACACTGCTAAA-3′). Following PCR amplification, products were subjected to BceAI digestion yielding band sizes of 467 bp for TrkA^{WT} (uncut) and 367 and 100 bp for the TrkA^{R685A} allele.

Adenoviral constructs. Recombinant adenoviruses expressing FLAG-TrkB:A^{F592A}-P2A-GFP or FLAG-TrkB:A$^{F592A/R685A}$-P2A-GFP, referred to as FLAG-TrkB:A-WT or FLAG-TrkB:A-R685A, respectively, were previously generated by subcloning into pAdenoX-Tet3G using the Adeno-X^{TM} Adenoviral System 3 kit (9). Recombinant adenoviral backbones were packaged into infectious adenoviral particles by transfection into human embryonic kidney cell line (HEK) 293 cells using polyethylenimine. High-titer viral stocks were purified using a CsCl gradient or VivaPure AdenoPack20 purification kit.

Live-cell antibody feeding. Live-cell antibody feeding assays to monitor Trk trafficking were performed as described previously (9). Sympathetic neurons isolated from P0 to P1 rat pups were grown in Campenot chambers for 9 d in vitro (DIV) until axons projected into the side compartments. Neurons were infected with doxycycline-inducible adenoviral vectors expressing FLAG-TrkB:A-WT or FLAG-TrkB:A-R685A chimeric receptors. Neurons were treated with 200 ng/mL doxycycline for 18 to 24 h to induce receptor expression. Infected neurons were identified by GFP that is coexpressed with the receptor using a self-cleaving P2A peptide sequence (GSGATNFSLLKQAGDVEENPGP). After withdrawing NGF from the culture media, surface chimeric receptors in axon compartments were labeled under live-cell conditions with a mouse anti-FLAG antibody (1:500) in phosphate-buffered saline (PBS) for 30 min at 4 °C. Excess antibody was washed off with PBS, followed by stimulation with BDNF (100 ng/mL) added to axon compartments in culture media at 37 °C for 20 min. Neurons were then placed on ice and briefly washed with ice-cold PBS, and axon compartments were washed twice in ice-cold acidic stripping buffer (0.3 N acetic acid, 1.5 M NaCl, pH 3.0) to remove surface anti-FLAG antibodies. Neurons were washed again with PBS and fixed with 4% paraformaldehyde (PFA) in PBS for 30 min at room temperature. Neurons were then permeabilized with 0.1% Triton X-100/5% normal goat serum/PBS and incubated with anti-mouse Alexa-546 secondary antibody (1:1,000; Thermo Scientific) for 2 h and then DAPI (0.3 μM) for 5 min followed by mounting on slides with Fluoromount Aqueous Mounting Medium (Sigma). In some experiments, axons were also visualized by immunostaining with anti-β-III-tubulin (1:1,000). To monitor retrograde trafficking of chimeric Trk receptors to cell bodies, the assays were performed as described above, except that axonal compartments were stimulated with BDNF (100 ng/mL) for 2 h without acid stripping of surface anti-FLAG antibodies from distal axon compartments.

Images of axons and cell bodies were acquired using a LSM700 confocal microscope. The same acquisition settings were applied to all images taken from a single experiment and analyzed by using ZEN 2012 (black edition) software. Axon images were captured as a snapshot of a single plane, and somas were captured in ~10-μm z-stacks. Intracellular accumulation of chimeric receptors was quantified as the number of FLAG-immunopositive punctae per cell body or axon. Neurons were visualized using the Green Fluorescent Protein (GFP) signal, and FLAG signals overlapping with GFP fluorescence were defined as internal receptors. For all imaging, a minimum of 10 cell bodies or axons were analyzed per condition per experiment. Results are expressed as means ± SEM and expressed relative to the "no ligand" condition.

Immunoblotting and immunoprecipitation. To assess TrkA phosphorylation and activation of downstream signaling, sympathetic neurons isolated from P0 to P3 TrkA^{WT} or TrkA^{R685A} mice were grown in mass cultures in NGF containing media for 4 DIV. After NGF deprivation for 24 h in the presence of BAF (50 μM), neurons were treated with NGF (100 ng/mL) for 30 min or culture media alone (no ligand condition). Neurons were lysed in 200 μL lysis buffer [20 mM Tris-HCl (pH 8.0), 150 mM NaCl, 10 mM NaF, 1 mM Na_3VO_4, 1 mM ethylenediaminetetraacetic acid (EDTA), 2 mm ethyleneglycoltetraacetic acid (EGTA), 1% Nonidet P40 detergent (NP-40), and cOmplete Mini protease inhibitor cocktail (Roche)], and total protein amounts estimated using Pierce bicinchoninic acid (BCA) assay and a microplate reader. After normalization for protein amounts, lysates were subjected to immunoblotting with anti-P-TrkA^{785} (1:1,000), followed by stripping and reprobing for P-Akt (1:1,000), then P-Erk1/2 (1:1,000), and last, p85 (1:1,000) as a loading control. All primary antibody incubations were done in Hikari signal enhancer buffer (Nacalai) and conducted overnight for ~16 h, followed by three washes with TBST (Tris-buffered saline and 0.1% Tween-20) and incubations with anti-mouse or anti-rabbit Horse Radish Peroxidase (HRP)-conjugated secondary antibodies for 1 h. Blots were then washed 3× in 5% milk/TBST and 3× in TBST prior to imaging. All immunoblots were visualized with ECL Plus Detection Reagent and scanned with a Typhoon 5 Variable Mode Imager (GE Healthcare). Results are expressed as means ± SEM and expressed relative to the "no ligand" condition.

To assess TrkA levels in sympathetic ganglia and axon terminals in vivo, SCGs and salivary glands were dissected from TrkA^{WT} or TrkA^{R685A} E16 mouse pups. SCG lysates were subjected to immunoblotting for anti-TrkA (1:1,000) or anti-p75 (1:1,000) in Hikari signal enhancer buffer (Nacalai), then stripped with Restore PLUS Western Blot Stripping Buffer (ThermoFisher), and reprobed for anti-β-III-tubulin (1:1,000). Salivary gland lysates were first subjected to TrkA immunoprecipitation using a mouse pan-Trk antibody (sc-7268). Immunoprecipitated samples were immunoblotted with rabbit anti-TrkA antibody, while input lysates were subjected to western blotting with an anti-β-III-tubulin (1:1,000) antibody. For some analyses, SCGs harvested from P0 TrkA^{WT} or TrkA^{R685A} mice were boiled in laemmli buffer and directly immunoblotted for P-TrkA^{Y785} (1:1,000), P-TrkA^{Y490} (1:1,000), or P-TrkA$^{Y674/675}$ (1:1,000). P-TrkA immunoblots were stripped and reprobed for total TrkA (1:1,000) and β-III-tubulin (1:1,000). Immunoblots were visualized with anti-rabbit or anti-mouse HRP-conjugated secondary antibodies. All immunoblots were visualized with ECL Plus Detection Reagent and scanned with a Typhoon 5 Variable Mode Imager (GE Healthcare). Results are means ± SEM from five to six mice per genotype and expressed relative to TrkA^{WT} mice.

Neuronal cell counts. Neuron counts were performed as previously described (9). In brief, torsos of E16, P0, P30, or P120 mice were fixed in 4%PFA/PBS for 4 h to overnight and cryoprotected in 30% sucrose/PBS for 24 to 48 h. P30 tissues were decalcified in 0.5 M EDTA prior to sucrose treatment. Torsos were then mounted in OCT and serially sectioned (12 μm). Next, every fifth section was stained with solution containing 0.5% cresyl violet (Nissl). Cells in both SCGs with characteristic neuronal morphology and visible nucleoli were counted using ImageJ.

Immunohistochemistry and TUNEL. Mouse torsos from E16, P0, P30, or P120 mice were fixed in 4% PFA/PBS, and tissue sections (12 μm) were permeabilized with PBS containing 0.1% Triton X-100 and blocked using 5% goat serum in PBS + 0.1% Triton X-100. Sections were then incubated with a rabbit anti-TH antibody (1:200), mouse anti-Tuj1 antibody (1:500), rabbit anti-TrkA antibody (1:200), rat anti-Ki67 antibody (1:200), or rabbit anti-cleaved caspase-3 antibody (1:200) overnight. For cleaved caspase-3, sections were first subjected to citrate antigen retrieval. Following PBS washes, sections were incubated with anti-rabbit or anti-mouse Alexa-488 secondary antibodies (1:500) and DAPI (0.3 μM). Sections were then washed in PBS and mounted in Fluoromount Aqueous Mounting Medium. TUNEL was performed according to the manufacturer's instructions using antigen retrieval methods. Images representing 6.3-μm optical slices were acquired using a Zeiss LSM 700 confocal scanning microscope with 405, 488-nm laser illumination. The same confocal acquisition settings were applied to all images taken from a single experiment. Quantification of sympathetic innervation was done by calculating integrated TH fluorescence density from multiple randomly selected images using ImageJ. Results are means ± SEM from three to five mice per genotype analyzed by a one-sample *t* test with hypothetical mean set at 100%. TUNEL^{+} and Ki67^{+} cells were counted and represented as a percentage of TH+-positive cells.

Axon growth. Sympathetic neurons isolated from P1 to P4 TrkA^{WT} or TrkA^{R685A} mice were grown in compartmentalized cultures (Campenot chambers) for 7 to 9 DIV. Neurons were either completely deprived of NGF or NGF (30 ng/mL) was added only to distal axons. BAF (50 μM) was also included to allow assessment of axon growth without the complications of cell death. Phase contrast images of axons were captured using a Retiga EXi camera in 24-h intervals for 3 d on a Zeiss Axiovert 200 microscope. Axon growth rate was measured using Openlab 4.0.4 for an average of 10 to 20 axons per condition. Axons were fixed in 4% PFA and stained with β-III-tubulin for representative images following experiments. Results are means ± SEM from three to four independent experiments and analyzed using the two-way ANOVA and Tukey–Kramer post hoc test.

Neuron survival. Sympathetic neurons from P1 to P4 TrkA^{WT} or TrkA^{R685A} mice were grown in compartmentalized cultures (Campenot chambers) for 7 to 9 DIV to allow axon projections to distal compartments. To ensure survival scoring of only the neurons that had projected axons into the axonal compartment, fluorescent microspheres (FluoSpheres™ carboxylate-modified microspheres, 0.04 μm)were added to the distal axon compartments 24 h before the experiments. Neurons were either starved of NGF (by adding anti-NGF at 1:1,000 dilution to both cell body and distal axon compartments) or supported by NGF (30 ng/mL) added only to distal axons. After 72 h, neurons were fixed, and dying cells were visualized using cleaved caspase-3 (1:200) immunostaining.

Neuronal apoptosis was calculated by determining the percentage of neurons that had extended axons into the side chambers (visualized by fluorescent microsphere uptake) that were also positive for the cleaved caspase-3 label.

Pupil analyses. Pupil size measurements were performed on 6- to 8-wk-old TrkA^{WT} or TrkA^{R685A} mice as reported previously (23). Briefly, all mice were dark-adapted and housed in single cages for 2 d and analyzed in the evenings. For all experiments, mice were unanesthetized and restrained by hand. To mitigate stress, which can affect pupil size, researchers handled mice for several days prior to the measurements. Videos of the eye were recorded for 30 s in the dark using a Sony 4K HD Video Recording FDRAX33 Handycam Camcorder mounted on a tripod at a fixed distance from the mouse. Manual focus was maintained on the camera to ensure that only one focal plane existed for each mouse. Pupil size was recorded under dim red light and the endogenous infrared light source of the camera to capture the basal pupil size. Results are means ± SEM from 7 TrkA^{WT} and 13 TrkA^{R685A} animals conducted across three independent experiments. The Student's *t* test was used for statistical analysis.

To assess pupillary light responses, TrkA^{R685A} or TrkA^{WT} littermates (6 to 8 wk old) were individually housed in the dark as above. Light stimulus was provided by a suspended 9- or 14-watt light bulb (Sunlite A19 Light Bulb, Daylight or Sunlite 80599-SU LED A19 Super Bright Light Bulb, Daylight). Neutral density filters (Roscolux) were used to filter out light to estimate log unit decreases in illumination. A luminometer (EXTECH Foot Candle/Lux Light Meter, 401025) was used to set the final luminescence (lux). Unanesthetized mice were restrained by hand in front of a mounted Sony 4K HD Video Recording FDRAX33 Handycam Camcorder in NightShot mode. Animals were held in front of the camera for 10 s to acquire basal pupil area under infrared light, and then, the light was switched on to visualize pupil constriction. Pupils were measured for 30 s. Animals were allowed to recover for 1 h in the dark between the measurements at different light intensities. Snapshots of the captured videos were taken using QuickTime player. Pupil area at the end of each 30-s time point was used to assess constriction. Results are means ± SEM from six TrkA^{WT} and five TrkA^{R685A} animals conducted across three independent experiments. The Student's *t* test was used for statistical analysis.

Ptosis. Six- to eight-week-old TrkA^{WT} or TrkA^{R685A} mice were dark-adapted and housed in single cages for 2 d. Unanesthetized mice were restrained by hand, and images of the eye taken using a Sony 4K HD Video Recording FDRAX33 Handycam Camcorder. Images were analyzed using ImageJ to measure the width and height of the eye surface and determine height/width ratio. Results are means ± SEM from 7 TrkA^{WT} and 13 TrkA^{R685A} animals conducted across three independent experiments. The Student's *t* test was used for statistical analysis.

Quantification and Statistical Analysis. Sample sizes were similar to those reported in previous publications (9, 36, 42). Data were collected randomly. For practical reasons, analyses of neuronal cell counts, axon growth, and axon innervation were done in a semiblinded manner such that the investigator was aware of the genotypes prior to the experiment but conducted the staining and data analyses without knowing the genotypes of each sample. All Student's *t* tests were performed assuming Gaussian distribution, two-tailed, unpaired, and a CI of 95%. Two-way ANOVAs with the post hoc Tukey test were performed when more than two groups were compared. Statistical analyses were based on at least three independent experiments and described in the figure legends. All error bars represent the SEM.

Data, Materials, and Software Availability. TrkA^{R685A} knock-in mice and adenoviral constructs generated in this study (*SI Appendix*, *Key Resources Table*) are available upon request. Microscopy data reported in this paper will be uploaded on BioImage Archive (https://www.ebi.ac.uk/bioimage-archive/submit/) upon acceptance. This paper does not report original code. Any additional information required to reanalyze the data reported in this paper is available from the lead contact upon request.

ACKNOWLEDGMENTS. We thank Haiqing Zhao for helpful comments on the manuscript. We also thank Haiqing Zhao for guidance in the design and generation of the TrkA^{R685A} knock-in mice. We thank Aurelia Mapps and Emily Scott-Solomon for consultations on pupil analyses and neuron survival/growth assays. We thank the Johns Hopkins University Transgenic Core Laboratory for help with generating the TrkA^{R685A} knock-in mice and the Johns Hopkins University Integrated Imaging Center for assistance with microscopy. This work was supported by NIH R01 awards, NS114478 and NS107342, to R.K. and NIH award F31 fellowship, NS113480, to B.C.

Author affiliations: [a]Department of Biology, Johns Hopkins University, Baltimore, MD 21218; and [b]Department of Applied Bioscience, Kanagawa Institute of Technology, Atsugi 243-0292, Japan

1. M. D. Horton, Ehlers, neuronal polarity and trafficking. *Neuron* **40**, 277–295 (2003).
2. I. Winckler, Mellman, trafficking guidance receptors. *Cold Spring Harb. Perspect. Biol.* **2**, a001826 (2010), 10.1101/cshperspect.a001826.
3. E. Scott-Solomon, R. Kuruvilla, Mechanisms of neurotrophin trafficking via Trk receptors. *Mol. Cell. Neurosci.* **91**, 25–33 (2018), 10.1016/j.mcn.2018.03.013.
4. A. W. Harrington, D. D. Ginty, Long-distance retrograde neurotrophic factor signalling in neurons. *Nat. Rev. Neurosci.* **14**, 177–187 (2013), 10.1038/nrn3253.
5. K. E. Cosker, R. A. Segal, Neuronal signaling through endocytosis. *Cold Spring Harb. Perspect. Biol.* **6**, a020669 (2014), 10.1101/cshperspect.a020669.
6. E. Scott-Solomon, E. Boehm, R. Kuruvilla, The sympathetic nervous system in development and disease. *Nat. Rev. Neurosci.* **22**, 685–702 (2021), 10.1038/s41583-021-00523-y.
7. K. Barford, C. Deppmann, B. Winckler, The neurotrophin receptor signaling endosome: Where trafficking meets signaling. *Dev. Neurobiol.* **77**, 405–418 (2017), 10.1002/dneu.22427.
8. M. Ascano, A. Richmond, P. Borden, R. Kuruvilla, Axonal targeting of Trk receptors via transcytosis regulates sensitivity to neurotrophin responses. *J. Neurosci.* **29**, 11674–11685 (2009), 10.1523/JNEUROSCI.1542-09.2009.
9. N. Yamashita, R. Joshi, S. Zhang, Z. Y. Zhang, R. Kuruvilla, Phospho-regulation of soma-to-axon transcytosis of neurotrophin receptors. *Dev. Cell* **42**, 626–639.e625 (2017), 10.1016/j.devcel.2017.08.009.
10. M. Stuible, M. L. Tremblay, In control at the ER: PTP1B and the down-regulation of RTKs by dephosphorylation and endocytosis. *Trends Cell Biol.* **20**, 672–679 (2010), 10.1016/j.tcb.2010.08.013.
11. C. Ozek, S. E. Kanoski, Z. Y. Zhang, H. J. Grill, K. K. Bence, Protein-tyrosine phosphatase 1B (PTP1B) is a novel regulator of central brain-derived neurotrophic factor and tropomyosin receptor kinase B (TrkB) signaling. *J. Biol. Chem.* **289**, 31682–31692 (2014), 10.1074/jbc.M114.603621.
12. N. Krishnan *et al.*, PTP1B inhibition suggests a therapeutic strategy for Rett syndrome. *J. Clin. Invest.* **125**, 3163–3177 (2015), 10.1172/JCI80323.
13. R. M. Stephens *et al.*, Trk receptors use redundant signal transduction pathways involving SHC and PLC-gamma 1 to mediate NGF responses. *Neuron* **12**, 691–705 (1994).
14. F. A. White *et al.*, Synchronous onset of NGF and TrkA survival dependence in developing dorsal root ganglia. *J. Neurosci.* **16**, 4662–4672 (1996).
15. Y. Ma, R. B. Campenot, F. D. Miller, Concentration-dependent regulation of neuronal gene expression by nerve growth factor. *J. Cell Biol.* **117**, 135–141 (1992), 10.1083/jcb.117.1.135.
16. H. Ye, R. Kuruvilla, L. S. Zweifel, D. D. Ginty, Evidence in support of signaling endosome-based retrograde survival of sympathetic neurons. *Neuron* **39**, 57–68 (2003).
17. A. Patel *et al.*, RCAN1 links impaired neurotrophin trafficking to aberrant development of the sympathetic nervous system in Down syndrome. *Nat. Commun.* **6**, 10119 (2015), 10.1038/ncomms10119.
18. R. J. Smeyne *et al.*, Severe sensory and sympathetic neuropathies in mice carrying a disrupted Trk/NGF receptor gene. *Nature* **368**, 246–249 (1994).
19. C. Crowley *et al.*, Mice lacking nerve growth factor display perinatal loss of sensory and sympathetic neurons yet develop basal forebrain cholinergic neurons. *Cell* **76**, 1001–1011 (1994).
20. T. J. Martin, Horner syndrome: A clinical review. *ACS Chem. Neurosci.* **9**, 177–186 (2018), 10.1021/acschemneuro.7b00405.
21. M. F. Goldberg, J. W. Payne, P. W. Brunt, Ophthalmologic studies of familial dysautonomia. The Riley-Day syndrome. *Arch. Ophthalmol.* **80**, 732–743 (1968), 10.1001/archopht.1968.00980050734011.
22. D. H. McDougal, P. D. Gamlin, Autonomic control of the eye. *Compr. Physiol.* **5**, 439–473 (2015), 10.1002/cphy.c140014.
23. W. T. Keenan *et al.*, A visual circuit uses complementary mechanisms to support transient and sustained pupil constriction. *eLife* **5**, e15392 (2016), 10.7554/eLife.15392.
24. A. M. Fagan *et al.*, TrkA, but not TrkC, receptors are essential for survival of sympathetic neurons in vivo. *J. Neurosci.* **16**, 6208–6218 (1996).
25. M. Shintani, Noda, protein tyrosine phosphatase receptor type Z dephosphorylates TrkA receptors and attenuates NGF-dependent neurite outgrowth of PC12 cells. *J. Biochem.* **144**, 259–266 (2008), 10.1093/jb/mvn064.
26. H. Tomita *et al.*, The protein tyrosine phosphatase receptor delta regulates developmental neurogenesis. *Cell Rep.* **30**, 215–228.e215 (2020), 10.1016/j.celrep.2019.11.033.
27. N. Arimura *et al.*, Anterograde transport of TrkB in axons is mediated by direct interaction with Slp1 and Rab27. *Dev. Cell* **16**, 675–686 (2009), 10.1016/j.devcel.2009.03.005.
28. C. B. Vaegter *et al.*, Sortilin associates with Trk receptors to enhance anterograde transport and neurotrophin signaling. *Nat. Neurosci.* **14**, 54–61 (2011), 10.1038/nn.2689.
29. Y. Tanaka *et al.*, The molecular motor KIF1A transports the TrkA neurotrophin receptor and is essential for sensory neuron survival and function. *Neuron* **90**, 1215–1229 (2016), 10.1016/j.neuron.2016.05.002.
30. E. E. Zahavi *et al.*, Combined kinesin-1 and kinesin-3 activity drives axonal trafficking of TrkB receptors in Rab6 carriers. *Dev. Cell* **56**, 1552–1554 (2021), 10.1016/j.devcel.2021.04.028.
31. D. D. Glebova, Ginty, growth and survival signals controlling sympathetic nervous system development. *Annu. Rev. Neurosci.* **28**, 191–222 (2005), 10.1146/annurev.neuro.28.061604.135659.
32. A. M. Fagan *et al.*, TrkA, but not TrkC, receptors are essential for survival of sympathetic neurons in vivo. *J. Neurosci.* **16**, 6208–6218 (1996).

33. P. J. Whitehouse *et al.*, Alzheimer's disease and senile dementia: Loss of neurons in the basal forebrain. *Science* **215**, 1237–1239 (1982), 10.1126/science.7058341.
34. M. V. Sofroniew, C. L. Howe, W. C. Mobley, Nerve growth factor signaling, neuroprotection, and neural repair. *Annu. Rev. Neurosci.* **24**, 1217–1281 (2001).
35. L. Zareen, A. Greene, Protocol for culturing sympathetic neurons from rat superior cervical ganglia (SCG). *J. Vis. Exp.* **23**, 988 (2009), 10.3791/988.
36. D. Bodmer, M. Ascano, R. Kuruvilla, Isoform-specific dephosphorylation of dynamin1 by calcineurin couples neurotrophin receptor endocytosis to axonal growth. *Neuron* **70**, 1085–1099 (2011), 10.1016/j.neuron.2011.04.025.
37. W. C. Mobley, A. Schenker, E. M. Shooter, Characterization and isolation of proteolytically modified nerve growth factor. *Biochem.* **15**, 5543–5551 (1976).
38. K. Labun, T. G. Montague, J. A. Gagnon, S. B. Thyme, E. Valen, CHOPCHOP v2: A web tool for the next generation of CRISPR genome engineering. *Nucleic Acids Res.* **44**, W272–W276 (2016), 10.1093/nar/gkw398.
39. S. H. Hough, A. Ajetunmobi, L. Brody, N. Humphryes-Kirilov, E. Perello, Desktop genetics. *Per. Med.* **13**, 517–521 (2016), 10.2217/pme-2016-0068.
40. J. G. Doench *et al.*, Optimized sgRNA design to maximize activity and minimize off-target effects of CRISPR-Cas9. *Nat. Biotechnol.* **34**, 184–191 (2016), 10.1038/nbt.3437.
41. P. D. Hsu *et al.*, DNA targeting specificity of RNA-guided Cas9 nucleases. *Nat. Biotechnol.* **31**, 827–832 (2013), 10.1038/nbt.2647.
42. E. Scott-Solomon, R. Kuruvilla, Prenylation of axonally translated Rac1 controls NGF-dependent axon growth. *Dev. Cell* **53**, 691–705.e697 (2020), 10.1016/j.devcel.2020.05.020.